ChemComm

COMMUNICATION

View Article Online
View Journal | View Issue

Cite this: *Chem. Commun.*, 2024, **60**, 12738

Received 24th August 2024,
Accepted 3rd October 2024

DOI: 10.1039/d4cc04305g

rsc.li/chemcomm

A two-dimensional coordination polymer with high laccase-like activity for sensitive colorimetric detection of thiram†

Songxue Han,[ab] Lili Xu,[bc] Youxing Fang*[b] and Shaojun Dong *[abc]

In contrast to natural enzymes, nanozymes show promising advantages of low cost and high stability for analytical applications. The simple mix of L-phenylalanine (F) and Cu^{2+} produces two-dimensional nanosheets of a coordination polymer with a high surface area ratio and rich exposed active sites as a novel catalyst. As the mimetic of natural laccase, this nanozyme (F–Cu) can catalyze the oxidative coupling reaction of 2,4-dichlorophenol (2,4-DP) and 4-aminoantipyrine (4-AP) to produce a distinct red product, thus establishing an intuitive and simple method for the detection of thiram. In the range of 0–7.5 μM, the absorbance intensity was linearly related to the concentration of thiram, and the detection limit was 0.0845 μM. The F–Cu nanozyme was successfully applied to the colorimetric detection of thiram in real samples.

As biological catalysts, natural enzymes efficiently catalyze various chemical reactions in living organisms, facilitating processes such as metabolism, nutrition, and energy conversion. However, the practical applications of natural enzymes are severely limited due to their inherent instability and high production costs.[1] Nanozymes, nanomaterials with enzyme-mimetic catalytic functions, have emerged as promising alternatives owing to their low cost and superior stability compared to natural enzymes.[2]

In recent years, the rapid development of nanozymes has benefited from the integration of nanotechnology and biological principles. Typical nanozymes exhibit catalytic activities similar to those of natural enzymes, such as peroxidases, oxidases, catalases, superoxide dismutases, and hydrolases. Nanozymes offer a series of advantages including structural diversity, tunable properties, remarkable stability, high specific surface area, simple preparation methods, and low cost, rendering them promising for diverse applications in areas such as chemical sensing, environmental monitoring and medical diagnostics.[3,4] Notably, nanozymes have demonstrated great potential as colorimetric sensors for the detection of various targets from small molecules to living organisms including glucose, phenols, toxicants, viruses and microorganisms.[5] Another unique feature of nanozymes is their potential recyclability, allowing them to retain catalytic activity after multiple uses. Despite significant advancements, designing an ideal nanozyme with exceptional catalytic activity and selectivity remains a challenge.

The rapid development of the chemical industry has led to widespread pollution from persistent organic compounds, posing significant threats to both human health and ecosystems. Typically, pesticide residues have raised huge concerns due to their adverse effects on ecological balance and human health. Among them, thiram is widely utilized as a protective agent for vegetables and grains, playing a crucial role in safeguarding agricultural productivity by controlling pests and weeds. However, thiram can contaminate water sources through runoff or accumulate in living organisms by permeating food chains, resulting in severe, irreversible, and persistent DNA damage, which poses a significant threat to ecological environments and human health.[6,7] Therefore, developing a convenient and simple method for detecting thiram residues is of critical importance.

Various analytical techniques have been employed for thiram detection, which can be categorized into optical methods, electrochemical methods, and chromatographic methods. Optical methods, including colorimetry,[8] fluorescence,[9] and surface enhanced Raman spectroscopy,[10] offer advantages of high sensitivity, rapidity, and ease of operation. Among them, colorimetric approaches distinguish themselves with their simplicity, cost-effectiveness, and intuitive visual readout, rendering them appealing for on-site analysis and field applications.[11] Recently, nanozyme based colorimetric assays have gained significant attention due to their unique advantages. Several nanozymes, such as single-atom nanozymes,[12] metal nanoclusters,[5] magnetic nanoparticles,[13] and metal–organic framework nanozymes,[14] have been successfully applied to colorimetric detection,[15] demonstrating great

[a] College of Chemistry, Jilin University, Changchun 130012, China
[b] State Key Laboratory of Electroanalytical Chemistry, Changchun Institute of Applied Chemistry, Chinese Academy of Sciences, Changchun 130022, China. E-mail: fangyx@ciac.ac.cn, dongsj@ciac.ac.cn
[c] University of Science and Technology of China, Hefei 230026, China

† Electronic supplementary information (ESI) available. See DOI: https://doi.org/10.1039/d4cc04305g

potential with their enzyme-like activities. These nanozyme based assays are not only low-cost and portable, but also simple to perform.[16] Despite advances in nanozyme-based colorimetric methods, many current approaches that rely on inhibiting nanozyme activity face challenges of low selectivity and poor differentiation between target analytes and interfering substances. Consequently, it is expected to develop highly sensitive colorimetric detection methods that leverage enhanced nanozyme catalytic activity to overcome these limitations.

In this work, we prepared F–Cu nanozymes with laccase-mimetic activity using Cu^{2+} and L-phenylalanine as precursors *via* a simple aqueous method.[17] Inspired by the catalytic mechanism of natural laccase, a copper-containing oxidase enzyme that catalyzes the oxidation of phenolic compounds, we developed a colorimetric method for thiram detection based on the laccase-like activity of F–Cu nanozymes. In this method, thiram enhances the nanozyme's catalytic activity, resulting in a distinctive color change in solution. The detection principle is illustrated in Scheme 1. Specifically, the F–Cu nanozyme catalyzes the oxidation of 2,4-dichlorophenol (2,4-DP) to produce hemiquinone radicals, which subsequently react with 4-aminoantipyrine (4-AP) to yield a colored product, 4-*N*-(1,4-benzoquinoneimine) antipyrine, with characteristic absorbance at 510 nm.[18] Within the range of 0–7.5 μM, the solution's absorbance intensity at 510 nm exhibited a linear correlation with thiram concentration, achieving a detection limit of 0.0845 μM. This approach was successfully applied for thiram analysis in actual water samples.

F–Cu nanosheet nanozymes were successfully synthesized using a spontaneous aqueous synthesis method described in a previous study.[17] The morphology of the F–Cu nanosheets was characterized by SEM (Fig. S1a and b, ESI†). It appeared as two-dimensional nanosheets with smooth surfaces, in agreement with prior results. AFM topography measurements revealed that the 2D crystal stacks can consist of multiple thin layers (Fig. S1c, ESI†), indicating that thicker stacks can be exfoliated into individual, thinner 2D nanosheets. The AFM topography image of the sonicated sample shows ultra-thin nanosheets with height of 2 nm, atomic monolayers. Additionally, the crystalline structures of F–Cu nanosheets were characterized by XRD, showing good agreement with literature patterns (Fig. S1d, ESI†). The obtained 2D nanosheets possess a high degree of crystallinity (10.55%). Energy-dispersive X-ray spectroscopy (EDX) analysis of the original sample revealed the presence of C, O, and Cu elements (Fig. S2a, ESI†). X-ray photoelectron spectroscopy (XPS) spectra in Fig. S2b (ESI†) further confirmed that F–Cu nanozymes were primarily composed of C, Cu, and O elements. The high-resolution XPS spectrum of Cu 2p in Fig. S2c (ESI†) shows the presence of Cu^{2+}, with peaks at 934.4 eV and 954.1 eV corresponding to Cu $2p_{3/2}$ and Cu $2p_{1/2}$ electrons of Cu^{2+}, respectively. Therefore, the synthesized F–Cu nanozymes were successfully prepared, containing only Cu^{2+} as confirmed by XPS and XRD results. F–Cu was further characterized by N_2 adsorption/desorption isotherm (Fig. S3, ESI†). The F–Cu had a large BET specific surface area (146.2 $m^2\ g^{-1}$) and pore volume (0.134 $cm^3\ g^{-1}$). The pore size distribution of F–Cu was predominantly concentrated in the mesoporous range, which facilitates the rapid transmission of mass, thus improving the catalytic performance of F–Cu.

Two-dimensional nanomaterials are expected to exhibit high activity due to their thin structure, which exposes the predominantly open structure on both sides of the sheets. Therefore, F–Cu was further evaluated for its laccase-like activity using the colorimetric reaction of 2,4-DP and 4-AP in PBS buffer, resulting in the formation of a red compound. During this process, 2,4-DP undergoes catalytic oxidation in the presence of F–Cu with laccase-like activity, and the resulting oxidation product reacts with 4-AP to generate a quinone-imine (QI), which exhibits maximum absorption at 510 nm.[18,19] The laccase activity of the nanozyme is directly proportional to the absorption intensity.

The impact of thiram on the laccase-like activity of F–Cu nanozymes was investigated. The laccase-like activity of F–Cu nanozyme showed a positive correlation with thiram concentration. As the concentration of thiram increased, the catalytic activity of the copper nanozymes was enhanced. Several controlled experiments were performed under varied conditions to demonstrate the enhanced catalytic activity of the nanozymes following the addition of thiram. As depicted in Fig. 2a, a mixture of thiram, 2,4-DP, and 4-AP showed minimal absorbance at 510 nm. The mixture of 2,4-DP and 4-AP exhibits negligible color and weak absorbance at 510 nm; however, upon addition of F–Cu nanozymes, the formation of a red product became detectable, and a dark pink color was generated when thiram was added (Fig. 1). These results suggest that thiram cannot promote the oxidation, but affect the activity of nanozymes. Thus, the enhancement of laccase-like activity could be attributed to the interaction between thiram and F–Cu nanozymes. To verify the catalytic activity of free Cu^{2+} or F–Cu, a comparative experiment was devised (Fig. S4, ESI†). The precipitate and supernatant obtained *via* centrifugation were separately mixed with a chromogenic substrate of 2,4-DP/4-AP for reaction. A light red color observed upon mixing the supernatant with the chromogenic substrate confirmed the

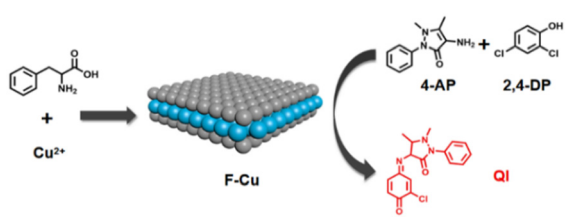

Scheme 1 Principle of colorimetric detection with F–Cu nanozymes.

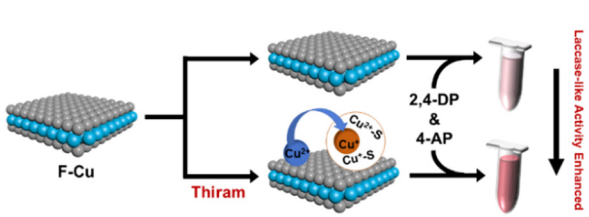

Fig. 1 Strategy of thiram detection based on F–Cu nanozymes.

moderate catalytic activity of free Cu^{2+}. Conversely, the mixture of the precipitation reaction with 2,4-DP/4-AP appeared dark pink, indicating the high catalytic activity of F–Cu. Thus, high laccase-like catalytic activity was demonstrated to originate from F–Cu rather than free Cu^{2+}.

Fig. 2b demonstrates that after the addition of thiram, 0.17% of the S element was detected in the F–Cu nanozyme by energy-dispersive X-ray spectroscopy (EDX), whereas no S element was detected in the original sample (Fig. S2a, ESI†). The XPS spectra of the Cu 2p region revealed that Cu^{2+} in F–Cu nanozymes was reduced to Cu^{+} and Cu–S bonds were formed. After the reaction, the XPS spectrum (Fig. 2c) of the F–Cu nanozyme exhibited peaks at 933.9 eV and 953.5 eV, corresponding to Cu $2p_{3/2}$ and Cu $2p_{1/2}$ electrons of Cu^{+}, respectively. These peaks were notably different from those observed in the original sample (Fig. S2c, ESI†). This phenomenon is attributed to the presence of reductive S element in thiram, which can reduce Cu^{2+} to Cu^{+}. XPS spectra (Fig. 2d) in the S 2p region also confirm the formation of Cu–S bonds between Cu and S. After the reaction, additional peaks at 163.1 eV and 161.9 eV were observed, which were absent in the original sample. These peaks correspond to the binding energies of S $2p_{1/2}$ and S $2p_{3/2}$ electrons, respectively, indicating the presence of Cu–S bonds. The enhanced catalytic activity of F–Cu nanozymes by thiram can be attributed to two factors. First, Cu^{2+} in F–Cu nanozymes was reduced to Cu^{+} and enhances laccase-like catalysis. Second, the formation of Cu–S bonds facilitates electron transfer, further improving the catalytic performance.[19]

Furthermore, unlike other common pesticides such as zineb and carbendazim, which reduce the activity of F–Cu nanozymes, thiram exhibits an enhanced effect on nanozyme activity with increasing concentrations. The experiment further confirmed that thiram specifically enhances the activity of F–Cu nanozymes, offering exceptional selectivity and promising application prospects for thiram detection.

We developed a colorimetric detection method for thiram based on F–Cu nanozymes and optimized the detection conditions, including pH and reaction temperature. The catalytic activity of F–Cu nanozymes was evaluated under various pH conditions in the absence of thiram (Fig. S5a, ESI†). Optimal performance was observed in a PBS buffered solution at pH 7.4. The impact of temperature on the measurement reaction was also investigated, and a reaction temperature of 60 °C was chosen (Fig. S5b, ESI†). The concentration of nanozymes was also assessed. The absorption intensity (A/A_0) of F–Cu reached a maximum at 6 mg mL^{-1} and remained stable with increasing concentration (Fig. S5c, ESI†). F–Cu nanozymes are also reusable and exhibit excellent stability. As depicted in Fig. S5d (ESI†), after 6 cycles, the catalytic activity remains nearly unchanged.

Under optimal conditions, thiram was detected by constructing a calibrated standard curve. It was observed that the maximum absorption at 510 nm increased as thiram concentration increased. Within the range of 0–7.5 μM, the absorption intensity at 510 nm exhibited a strong linear correlation with thiram concentration (Fig. 3a). The detection limit was 0.0845 μM (3σ). Table S1 (ESI†) provides a comparative analysis of the different detection methods of thiram. The colorimetric assay developed in this study demonstrated a better LOD and wider linear range compared to Method 2, 3, and 4. The practical implementation of Method 1, 5, and 6 is hindered by the need for precision instrumentation and high maintenance costs. In contrast, our method designed in this experiment provides a more cost-effective, feasible, and user-friendly solution compared to alternative methods, suggesting the feasibility of F–Cu nanozyme-based sensing of thiram.

The laccase-like steady-state kinetic parameters of F–Cu nanozymes using thiram as the substrate were investigated. The initial rate of the catalytic reaction was measured, and the

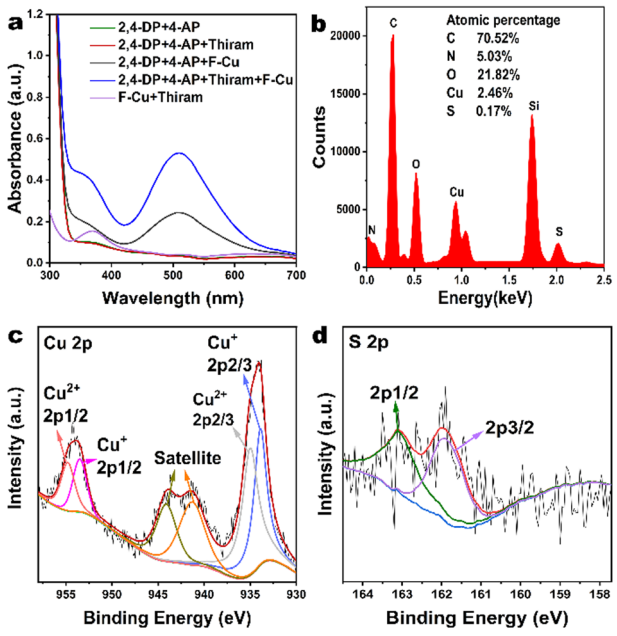

Fig. 2 (a) Validation of the laccase-like activity of F–Cu nanozymes. (b) EDX spectrum of F–Cu nanozyme in the presence of thiram. (c) Cu 2p and (d) S 2p XPS spectra and peak fitting by XPS peak-differentiating-imitating analysis of F–Cu nanozymes in the presence of thiram.

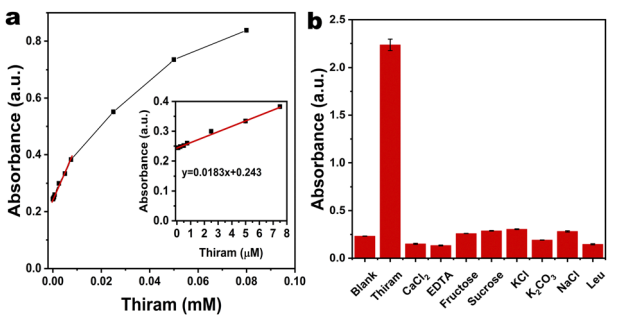

Fig. 3 (a) Absorbance at 510 nm of F–Cu nanozymes reacting with different concentrations of thiram. The reaction was carried out in pH 7.4 PBS buffer. (b) Response of the system catalyzed by F–Cu nanozymes to thiram and potential interfering substances, including inorganic ions, biomolecules, and reducing agents.

apparent kinetic parameter was calculated using the Lineweaver–Burk diagram (Fig. 3a):

$$V = V_m \times [S]/(K_m + [S]) \quad (1)$$

$$1/V = K_m/V_m(1/[S]) + 1/V_m \quad (2)$$

The Michaelis constant (K_m) can be determined from the Michaelis–Menten kinetic equation (eqn (1)) and Lineweaver–Burk plot (eqn (2)), where V represents the initial velocity, V_m denotes the maximum reaction rate, [S] stands for the substrate concentration, and K_m is the Michaelis constant. *A* smaller K_m value indicates higher enzyme activity.

To evaluate the interference resistance of the detection method, sodium chloride, potassium chloride, fructose, sucrose, leucine, potassium carbonate, and edetate disodium were chosen as the interferents (Fig. 3b). Thiram significantly increased the absorption intensity under the experimental conditions, while the interferents did not notably affect the activity of F–Cu nanozymes. These results demonstrate that the detection method exhibits excellent selectivity and interference resistance.

To evaluate the practical applicability of the F–Cu nanozyme-based method, we assessed its performance in detecting thiram in lake and river water samples. This assessment is crucial, as thiram can contaminate water sources or enter the food chain, potentially causing severe, irreversible, and persistent DNA damage in animals and humans, thus posing a significant threat to both ecological systems and human health. Lake and river water samples were pre-treated by centrifugation (10 000 rpm, 5 min) and filtration through a 0.5 μm membrane to remove insoluble matter. Various concentrations of thiram were then spiked into these samples to determine the method's recovery rates and relative standard deviation (RSD) values. As presented in Table S2 (ESI†), the recovery rates were 101.2–118.4% and 118–121.8%, with RSD values between 1.93% and 2.42% and 1.57–2.37%, respectively. These results demonstrate the high accuracy and precision of the F–Cu nanozyme-based method, indicating its promising potential for practical applications in environmental monitoring and food safety.

In summary, we synthesized 2D F–Cu nanosheet nanozymes with laccase-mimetic activity *via* a simple aqueous route using copper chloride and L-phenylalanine as precursors. By leveraging the enhanced laccase-like catalytic activity of F–Cu nanozymes in the presence of thiram, we developed a straightforward and sensitive colorimetric method for thiram detection. This approach demonstrated excellent selectivity, as thiram specifically enhances the nanozyme's catalytic performance, resulting in a distinctive color change, while common coexisting species showed negligible interference. Within a linear range of 0–7.5 μM, the solution's absorbance intensity at 510 nm increased proportionally with thiram concentration, achieving a low detection limit of 0.0845 μM. The mechanism behind this activity enhancement involves two key factors: the reduction of Cu^{2+} to Cu^{+} in the nanozyme by thiram, and the formation of Cu–S bonds that promote electron transfer, synergistically increasing the catalytic activity. This dual effect contributes to the high selectivity and sensitivity of the analytical method, allowing for reliable thiram detection even in complex sample matrices. Importantly, we confirmed the practical applicability of this nanozyme-based assay by successfully detecting thiram in real water samples. These findings highlight the potential of our method for environmental monitoring and analysis, offering a practical tool for addressing challenges in water quality assessment and food safety.

This work was financially supported by the Science and Technology Development Plan Project of Jilin Province (SKL202302032), China and the National Natural Science Foundation of China (No. 22274149 and 22074137).

Data availability

The data supporting this article have been included as part of the ESI.†

Conflicts of interest

There are no conflicts to declare.

Notes and references

1 L. Alvarado-Ramírez, G. Machorro-García, A. López-Legarrea, D. Trejo-Ayala, M. D. J. Rostro-Alanis, M. Sánchez-Sánchez, R. M. Blanco, J. Rodríguez-Rodríguez and R. Parra-Saldívar, *Biotechnol. Adv.*, 2024, **70**, 108299.
2 M. Li, J. Chen, W. Wu, Y. Fang and S. Dong, *J. Am. Chem. Soc.*, 2020, **142**, 15569–15574.
3 R. M. Rego, G. Sriram, K. V. Ajeya, H.-Y. Jung, M. D. Kurkuri and M. Kigga, *J. Hazard. Mater.*, 2021, **416**, 125941.
4 N. Garg, A. Deep and A. L. Sharma, *Coord. Chem. Rev.*, 2021, **445**, 214073.
5 N. Gao, J. Xu, X. Li, G. Ling and P. Zhang, *Chem. Eng. J.*, 2023, **465**, 142817.
6 S. Li, J. Wu, S. Zhang, T. Jiao, J. Wei, X. Chen, Q. Chen and Q. Chen, *Food Chem.*, 2024, **434**, 137438.
7 B. Rai and S. D. Mercurio, *Environ. Sci. Pollut. Res.*, 2020, **27**, 10629–10641.
8 H. Sun, Q. Mei, S. Shikha, J. Liu, J. Zhang and Y. Zhang, *Microchim. Acta*, 2019, **186**, 106.
9 F. Wang, Z. Li, H. Jia, C. Miao, R. Lu, S. Zhang and Z. Zhang, *Food Chem.*, 2023, **409**, 135328.
10 M. B. Bhavvya, B. R. Prabhu, A. Tripathi, S. Yadav, N. S. John, R. Thapa, A. Altaee, M. Saxena and A. K. Samal, *ACS Sustainable Chem. Eng.*, 2022, **10**, 7330–7340.
11 M. Nazifi, A. M. Ramezani, G. Absalan and R. Ahmadi, *Sens. Actuators, B*, 2021, **332**, 129459.
12 Z. Lyu, J. Zhou, S. Ding, D. Du, J. Wang, Y. Liu and Y. Lin, *TrAC, Trends Anal. Chem.*, 2023, **168**, 117280.
13 M.-L. Ye, Y. Zhu, Y. Lu, L. Gan, Y. Zhang and Y.-G. Zhao, *Talanta*, 2021, **230**, 122299.
14 L. Zhang, X. Bi, X. Liu, Y. He, L. Li and T. You, *Nanoscale*, 2023, **15**, 12853–12867.
15 Z. Su, T. Du, X. Liang, X. Wang, L. Zhao, J. Sun, J. Wang and W. Zhang, *Food Control*, 2022, **141**, 109165.
16 Z. Chi, Q. Wang and J. Gu, *Analyst*, 2023, **148**, 487–506.
17 P. Makam, S. S. R. K. C. Yamijala, V. S. Bhadram, L. J. W. Shimon, B. M. Wong and E. Gazit, *Nat. Commun.*, 2022, **13**, 1505.
18 H. Y. Kim, H. J. Lee and S.-K. Chang, *Talanta*, 2015, **132**, 625–629.
19 X. Zhang, D. Wu, Y. Wu and G. Li, *Biosens. Bioelectron.*, 2021, **172**, 112776.